

## Chapter 21

### Niobium Oxalate

#### New Precursor for Preparation of Supported Niobium Oxide Catalysts

Jih-Mirn Jehng and Israel E. Wachs

Zettlemoyer Center for Surface Studies, Department of Chemical Engineering, Lehigh University, Bethlehem, PA 18015

The aqueous preparation of supported niobium oxide catalysts was developed by using niobium oxalate as a precursor. The molecular states of aqueous niobium oxalate solutions were investigated by Raman spectroscopy as a function of pH. The results show that two kinds of niobium ionic species exist in solution and their relative concentrations depend on the solution pH and the oxalic acid concentration. The supported niobium oxide catalysts were prepared by the incipient wetness impregnation technique and characterized by Raman, XRD, XPS, and FTIR as a function of niobium oxide coverage and calcination temperature. The Raman studies reveal that two types of surface niobium oxide species exist on the alumina support and their relative concentrations depend on niobium oxide coverage. Raman, XRD, XPS, and FTIR results indicate that a monolayer of surface niobium oxide corresponds to ~ 19% Nb<sub>2</sub>O<sub>5</sub> for an Al<sub>2</sub>O<sub>3</sub> support possessing ~ 180 m<sup>2</sup>/g. The surface niobium oxide phase is found to be stable to high calcination temperatures.

Supported niobium oxide catalysts have recently been shown to be effective catalysts for many catalytic reactions: pollution abatement, selective oxidation, hydrocarbon conversion, carbon monoxide hydrogenation, etc. [1]. In a previous study [2], it was shown that the presence of the surface niobium oxide phases retards the loss in surface area of the Al<sub>2</sub>O<sub>3</sub> and TiO<sub>2</sub> supports and stabilizes the V<sub>2</sub>O<sub>5</sub>/TiO<sub>2</sub> system during high temperature treatments. The surface niobium oxide species on the Al<sub>2</sub>O<sub>3</sub> support was also found to possess

0097-6156/90/0437-0232\$06.00/0  
© 1990 American Chemical Society

strong Bronsted acidity [3]. These important properties impart the surface niobium oxide phase on the  $\text{Al}_2\text{O}_3$  support with a high hydrocarbon cracking activity at elevated temperatures.

Niobium ethoxide  $[\text{Nb}(\text{OC}_2\text{H}_5)_5]$  has traditionally been used as a precursor for the preparation of supported niobium oxide catalysts. This non-aqueous preparation method requires a controlled environment and special procedures to avoid the decomposition of the niobium ethoxide in the presence of moisture. It is well-known that transition metal ions form a stable solution chelate with oxalate groups, and molybdenum oxalate [4] and vanadium oxalate [5] have been widely used for the aqueous preparation of supported molybdenum oxide and supported vanadium oxide catalysts. In the present study, niobium oxalate  $[\text{Nb}(\text{HC}_2\text{O}_4)_5]$  was investigated as an aqueous precursor for the preparation of supported niobium oxide catalysts.

## EXPERIMENTAL METHODS

### Materials and Preparation Methods

Niobium oxalate was supplied by Niobium Products Company with the following chemical analysis: 20.5%  $\text{Nb}_2\text{O}_5$ , 790 ppm Fe, 680 ppm Si, and 0.1% insolubles. Niobium oxalate was dissolved into a constant concentration of aqueous oxalic acid solution, and the pH of the solution was varied from 0.50 to 5.00 by adding ammonium hydroxide. The supported niobium oxide on  $\text{Al}_2\text{O}_3$  catalysts were prepared by the incipient-wetness impregnation method using the niobium oxalate/oxalic acid aqueous solution and  $\text{Al}_2\text{O}_3$  (Harshaw, 180  $\text{m}^2/\text{g}$ ). The samples were dried at 110–120°C for 16 hours, and then calcined at 500°C under flowing dry air for 16 hours.

### Raman Spectroscopy

Raman spectra were obtained with a Spex Triplemate spectrometer (Model 1877) coupled to an EG&G intensified photodiode array detector cooled thermoelectrically to -40°C, and interfaced with an EG&G OMA III Optical Multichannel Analyzer (Model 1463). The samples were excited with the 514.5nm  $\text{Ar}^+$  laser. The beam was focused on the sample illuminator where the sample typically spins at about 2000 rpm to avoid local heating. The Raman scattering was collected by the spectrometer, and analyzed with an OMA III built-in software package. The overall spectral resolution of the spectra is about 2  $\text{cm}^{-1}$ .

### X-Ray Powder Diffraction (XRD)

The crystalline  $\text{Nb}_2\text{O}_5$  phase in the supported niobium oxide catalysts was detected by an APD 3600 automated X-

ray powdered diffractometer using Cu  $K_{\alpha}$  (45KV, 30MA) radiation. The  $Nb_2O_5/Al_2O_3$  samples were calcined at 700°C to increase the  $Nb_2O_5$  particle size and enhance the XRD signals.

### X-Ray Photoelectron Spectroscopy (XPS)

XPS experiments were performed on a Physical Electronic Instruments ESCA/AUGER system. The samples were placed on the sample holder at a 45° angle to the entrance of analyzer and the system was evacuated to  $10^{-9}$  -  $10^{-10}$  Torr. The XPS spectra were calibrated against the Au 4f<sub>7/2</sub> peak using the Mg  $K_{\alpha}$  line as the X-ray exciting radiation.

### CO<sub>2</sub> Chemisorption

The CO<sub>2</sub> uptake of supported niobium oxide on Al<sub>2</sub>O<sub>3</sub> at different Nb<sub>2</sub>O<sub>5</sub> loadings was measured with a Quantasorb BET apparatus using a 1:9 ratio of CO<sub>2</sub>/He mixture gases. The samples were degassed at 250°C for 2 hours under flowing He, and the CO<sub>2</sub> chemisorption was performed at room temperature.

## RESULTS AND DISCUSSION

### Niobium oxide reference compounds

The Raman spectra of several niobium oxide compounds, with their corresponding symmetry and coordination, are shown in Figure 1. The  $Nb_6O_{19}^{-8}$  unit is a well-characterized structure which consists of three different types of Nb-O bonds at each niobium center: a short Nb=O terminal double bond, a longer Nb-O-Nb bridging bond, and a very long and weak Nb---O single bond connected to the center of the cage-like octahedral structure [6-8]. From the known structure of  $K_8Nb_6O_{19}$  the main frequencies of the  $K_8Nb_6O_{19}$  Raman spectrum in Figure 1 can be assigned: Nb=O terminal stretching mode (903, 879, and 831  $cm^{-1}$ ), corner or edge-shared octahedral  $NbO_6$  stretching mode (734, 537, and 463  $cm^{-1}$ ), Nb=O bending mode (289  $cm^{-1}$ ), and Nb-O-Nb bending mode (223  $cm^{-1}$ ). The multiple terminal stretching modes present in the high wavenumber region are due to distortions present in the  $K_8Nb_6O_{19}$  structure. Niobium pentoxide,  $Nb_2O_5$ , possesses a more order octahedral structure with no Nb=O terminal bonds, and a major band appears at 690  $cm^{-1}$  which is characteristic of an octahedral  $NbO_6$  stretching mode as well as Nb-O and Nb-O-Nb bending modes at ~300  $cm^{-1}$  and ~230  $cm^{-1}$ , respectively. For the niobium oxalate precursor a sharp and strong Raman band is present at 958  $cm^{-1}$  due to a Nb=O terminal bond and the associated bending modes appear in the 200-400  $cm^{-1}$  region. The Raman band at

$\sim 570$   $\text{cm}^{-1}$  arises from the bidentate oxalate ligands coordinated to the niobium [9,10]. The Raman frequencies of the reference compounds are tabulated in Table 1.

### Niobium Oxalate Aqueous Solutions

Niobium oxalate has a low solubility in aqueous solutions, but its solubility can be dramatically increased by the addition of oxalic acid to the aqueous solutions. At high oxalic acid concentrations, however, the niobium oxalate and oxalic acid precipitate from solution. The solubility curve of niobium oxalate in aqueous solutions is shown in Figure 2 as a function of the oxalic acid concentrations. Figure 3 shows a series of Raman spectra of the niobium oxalate in aqueous oxalic acid solutions with varying pH (0.50 to 5.00). At low pH ( $<3.00$ ), Two peaks are observed in the 900-1000  $\text{cm}^{-1}$  region which are characteristic of Nb=O terminal stretching modes. The behavior of these two peaks with pH variation suggests that two niobium oxalate species exist in solution. The associated bending modes appear in 200-400  $\text{cm}^{-1}$  region. A Nb-O<sub>2</sub>-C<sub>2</sub> breathing mode also appears at  $\sim 570$   $\text{cm}^{-1}$ . At high pH ( $>5.00$ ), two new Raman bands form at  $\sim 670$   $\text{cm}^{-1}$  and  $\sim 220$   $\text{cm}^{-1}$  which indicate the formation of hydrated Nb<sub>2</sub>O<sub>5</sub>.

It is known that the niobium oxide complexes in oxalic acid aqueous solutions display an equilibria between two ionic species containing 2 or 3 oxalate groups which depend on the solution pH and the oxalic acid concentration [11,12]. Thus, the two Nb=O terminal bonds appearing in the aqueous Raman spectra are assigned to the two different niobium oxalate ionic species present in the solution. The Raman spectra also show that the relative intensity of two Nb=O bands,  $\sim 910$   $\text{cm}^{-1}$  and  $\sim 930$   $\text{cm}^{-1}$ , changes with increasing pH. When ammonium hydroxide is added to the solution, the niobium oxalate species with 3 oxalate groups starts to hydrolyze to 2 oxalate groups as one of the oxalate groups is replaced by OH groups. This results in an increase in intensity of the  $\sim 910$   $\text{cm}^{-1}$  Nb=O band with increasing solution pH. Increasing the pH to about 5.00 by further addition of ammonium hydroxide causes the niobium oxalate species to hydrolyze and coagulate to a hydrated Nb<sub>2</sub>O<sub>5</sub> precipitate. The aqueous solution chemistry of niobium oxalate is shown below:

Table 1: Raman frequencies of bulk niobium oxide compounds

Vibrational Modes	Wavenumber ( $\text{cm}^{-1}$ )		
	$\text{K}_8\text{Nb}_6\text{O}_{19}$	$\text{Nb}_2\text{O}_5$	$\text{Nb}(\text{HC}_2\text{O}_4)_5$
$\nu(\text{Nb}=\text{O})$	903,879,831	-	958
$\nu(\text{NbO}_6)$	734 537 463	690	-
$\nu(\text{NbO}_2\text{C}_2)$	-	-	572
$\delta(\text{Nb}-\text{O})$	289	302	284
$\delta(\text{Nb}-\text{O}-\text{Nb})$	223	238	243

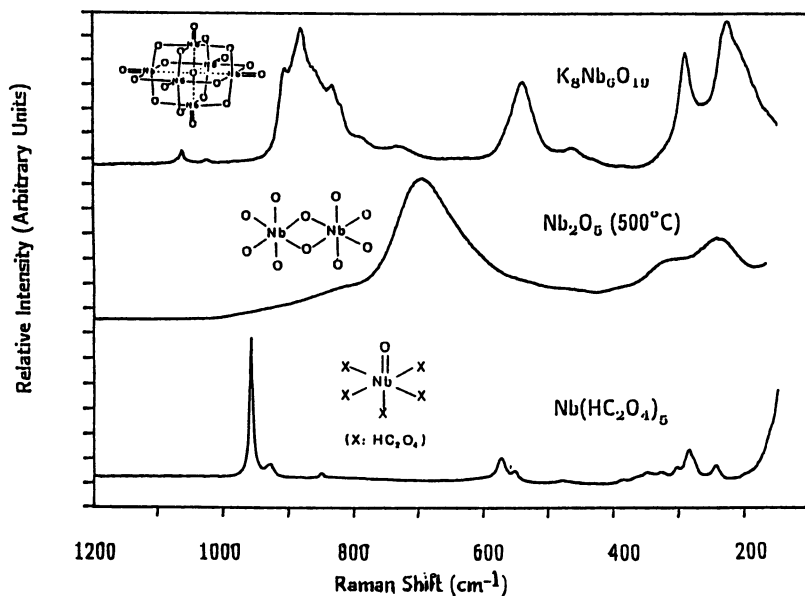


Figure 1: The solubility of niobium oxalate in solution as a function of oxalic acid added.

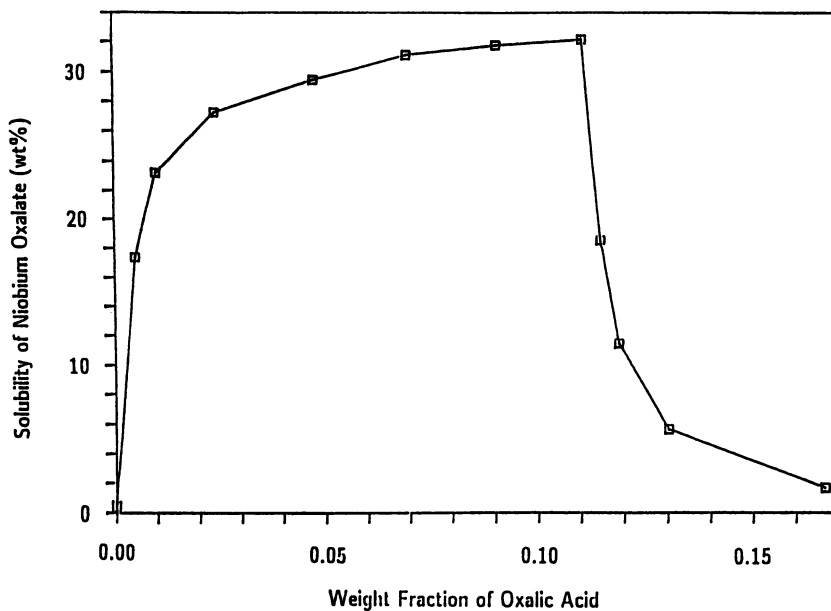


Figure 2: Raman spectra of bulk niobium oxide compounds.

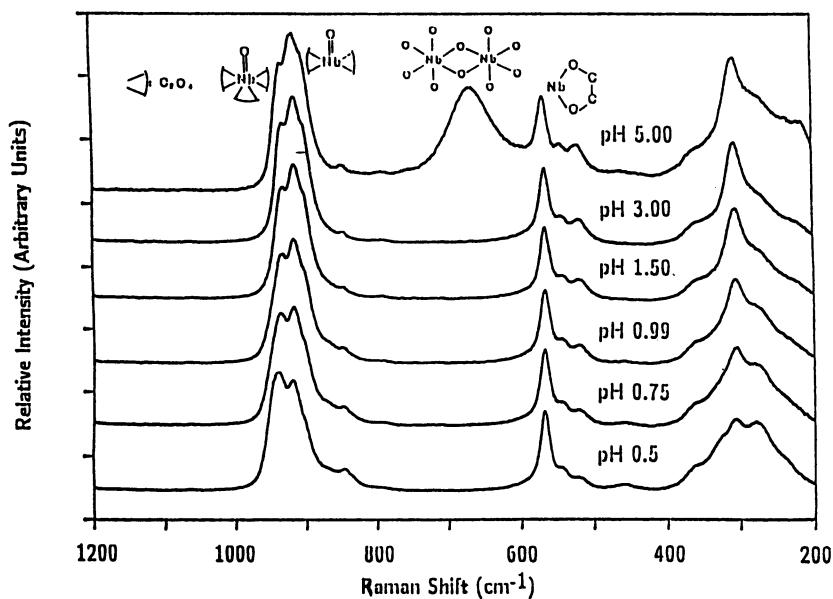
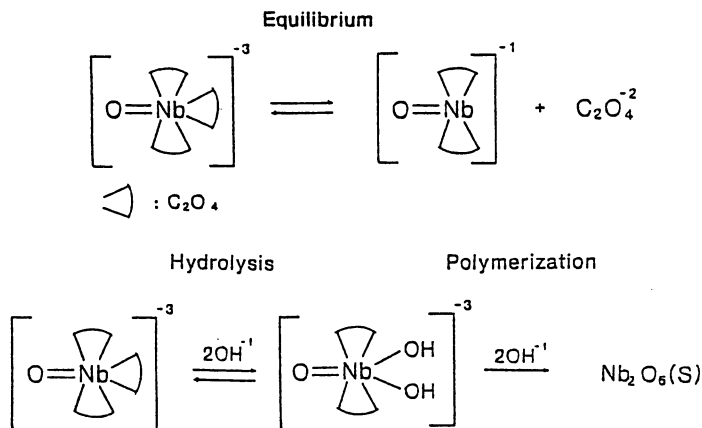


Figure 3: Raman spectra of niobium oxalate in oxalic acid solution as a function of pH from 0.5 to 5.00.



### Supported Niobium Oxide on Alumina

The Raman spectra of supported niobium oxide on alumina are shown in Figure 4 as a function of  $\text{Nb}_2\text{O}_5$  loading. The nature of the supported niobium oxide phase is determined by comparison of the Raman spectra of the supported niobium oxide samples with those of niobium oxide reference compounds. The Raman features of 1-22%  $\text{Nb}_2\text{O}_5/\text{Al}_2\text{O}_3$  samples are different than the bulk niobium oxide compounds due to the formation of a two-dimensional surface niobium oxide overlayer on the alumina support [2]. At low surface coverages (<8%  $\text{Nb}_2\text{O}_5/\text{Al}_2\text{O}_3$ ), the weak and broad Raman band in the 890-910  $\text{cm}^{-1}$  region is present due to a distorted octahedral (approaching square-pyramidal) surface niobium oxide species possessing Nb=O bonds, and the mode at  $\sim 230 \text{ cm}^{-1}$  is characteristic of a Nb-O-Nb linkage. At high surface coverages (>8%  $\text{Nb}_2\text{O}_5/\text{Al}_2\text{O}_3$ ), an additional Raman band at  $\sim 630 \text{ cm}^{-1}$  is also present due to a slightly distorted octahedral surface niobium oxide species. The Raman studies reveal that two types of surface niobium oxide species exist on the alumina support, and that their relative concentrations depend on the surface niobium oxide coverage.

A series of supported niobium oxide on alumina catalysts, 0-45%  $\text{Nb}_2\text{O}_5/\text{Al}_2\text{O}_3$ , were further characterized by XRD, XPS,  $\text{CO}_2$  chemisorption, as well as Raman spectroscopy in order to determine the monolayer content of the  $\text{Nb}_2\text{O}_5/\text{Al}_2\text{O}_3$  system. The transition from a two-dimensional metal oxide overlayer to three-dimensional metal oxide particles can be detected by monitoring the

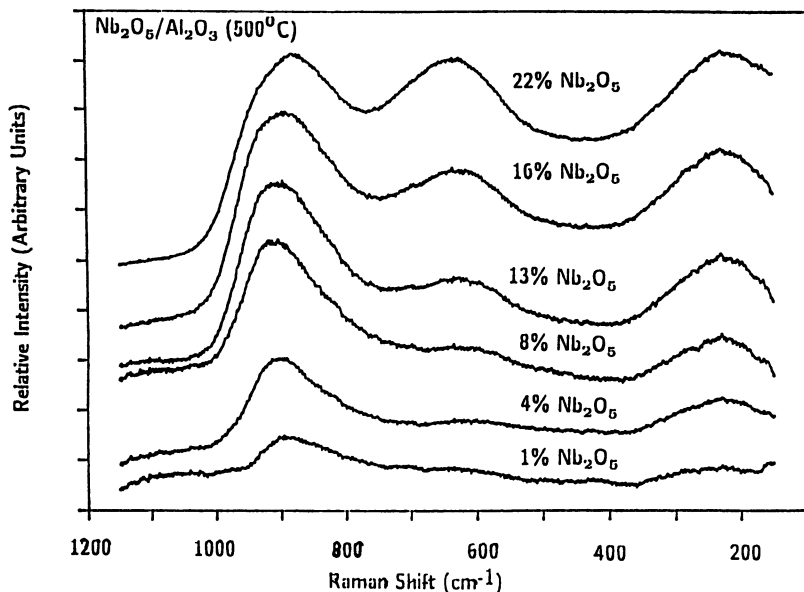


Figure 4: Raman spectra of  $\text{Nb}_2\text{O}_5/\text{Al}_2\text{O}_3$  (500°C) as a function of niobium oxide coverage.

$(\text{Nb}/\text{Al})_{\text{surface}}$  ratios in such systems with XPS because of the vastly different XPS cross-sections of these two phases [13]. The  $(\text{Nb}/\text{Al})_{\text{surface}}$  ratios of the niobium oxide on the alumina support were obtained by integrating the areas of the Nb 3d<sub>3/2,5/2</sub> and the Al 2p photoelectron lines, and the  $(\text{Nb}/\text{Al})_{\text{surface}}$  vs.  $(\text{Nb}/\text{Al})_{\text{bulk}}$  curve is shown in Figure 5. The surface break in the curve corresponds to ~19%  $\text{Nb}_2\text{O}_5/\text{Al}_2\text{O}_3$  and suggests that the transition from a two-dimensional phase to three-dimensional particles, monolayer coverage, occurs at this point. This conclusion is supported by XRD measurements which only detect crystalline  $\text{Nb}_2\text{O}_5$  particles above 19%  $\text{Nb}_2\text{O}_5/\text{Al}_2\text{O}_3$ , and  $\text{CO}_2$  chemisorption measurements (see Figure 6) which indicate that the basic alumina hydroxyls have been removed by the niobium oxide overlayer [14,15]. The slight increase in the  $\text{CO}_2$  chemisorption above 19%  $\text{Nb}_2\text{O}_5/\text{Al}_2\text{O}_3$  is due to  $\text{CO}_2$  chemisorption on the crystalline  $\text{Nb}_2\text{O}_5$  particles. The Raman spectra in Figure 7 reveal that the 630  $\text{cm}^{-1}$  band of the surface niobium oxide phase begins to shift towards the 690  $\text{cm}^{-1}$  band of crystalline  $\text{Nb}_2\text{O}_5$  above 19%  $\text{Nb}_2\text{O}_5/\text{Al}_2\text{O}_3$  due to the presence of crystalline  $\text{Nb}_2\text{O}_5$  particles. Thus, XPS, XRD,  $\text{CO}_2$  chemisorption, and Raman all demonstrate that a monolayer of surface niobium oxide on alumina, ~180  $\text{m}^2/\text{g}$ , corresponds to ~19%  $\text{Nb}_2\text{O}_5/\text{Al}_2\text{O}_3$ .



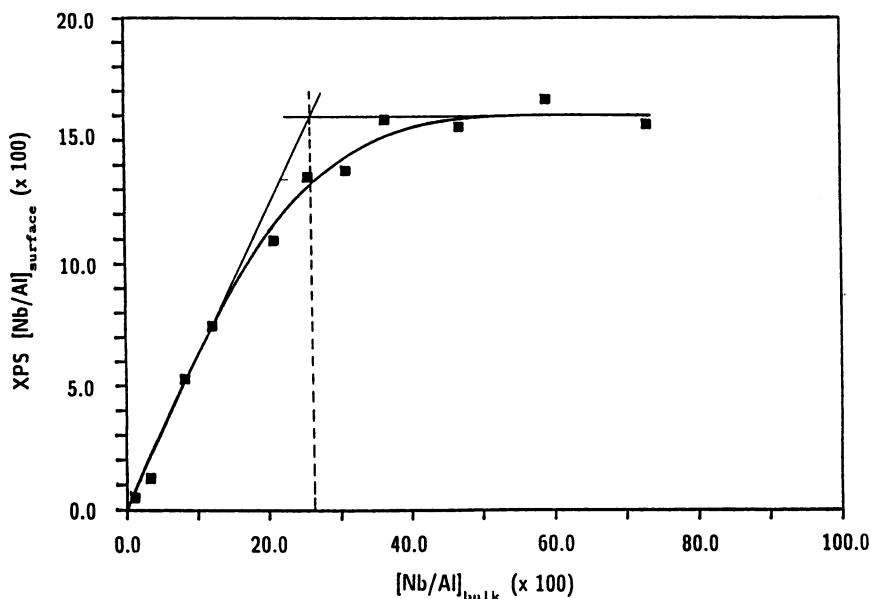


Figure 5: Raman shifts of  $\text{Nb}_2\text{O}_5/\text{Al}_2\text{O}_3$  ( $700^\circ\text{C}$ ) as a function of niobium oxide coverage.

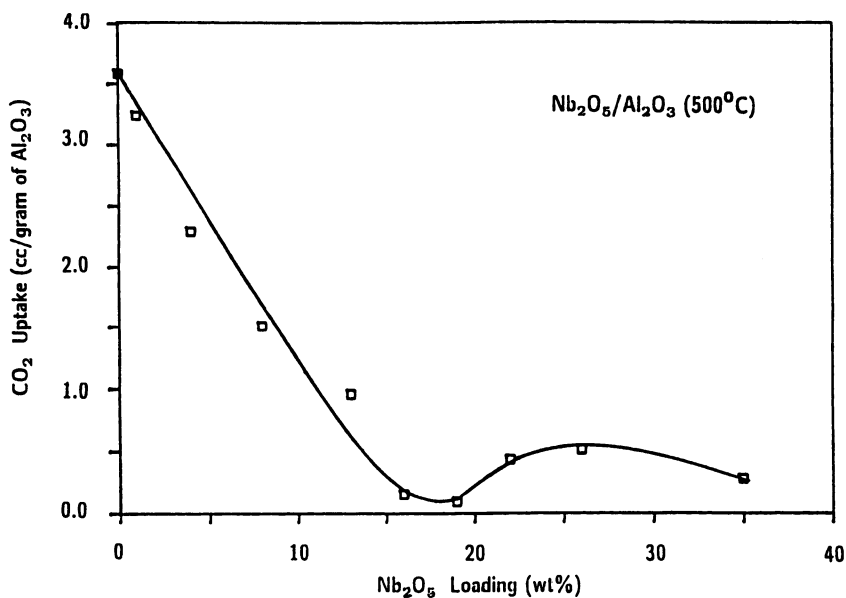


Figure 6: XPS intensity ratios of  $(\text{Nb}/\text{Al})_{\text{surface}}$  as a function of  $(\text{Nb}/\text{Al})_{\text{bulk}}$ .

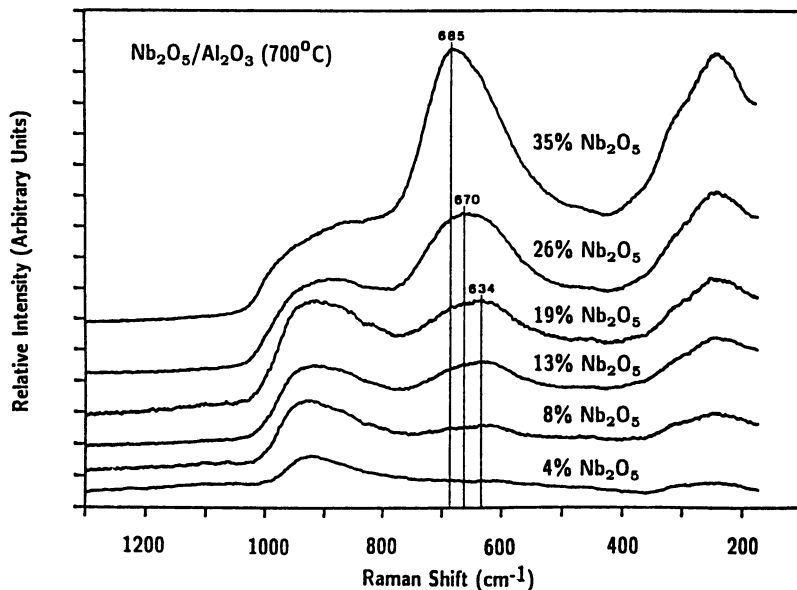


Figure 7:  $\text{CO}_2$  uptake of  $\text{Nb}_2\text{O}_5/\text{Al}_2\text{O}_3$  ( $500^\circ\text{C}$ ) as a function of niobium oxide coverage.

### ACKNOWLEDGMENTS

The support of Niobium Products Company for this research project is gratefully acknowledged.

### REFERENCES

1. Niobium Products Company Inc., Catalytic Applications of Niobium
2. J. M. Jehng, F. D. Hardcastle, and I. E. Wachs, Solid State Ionics, 32/33, 904(1989)
3. L. L. Murrell, D. C. Grenoble, C. J. Kim, and N. C. Dispenziere, Jr., J. Catal. 107, 463, (1987)
4. K. Y. Ng, X. Zhou, and E. Gulari, J. Phys. Chem. 89, 2477, (1985)
5. R. Y. Saleh, I. E. Wachs, S. S. Chan, and C. C. Chersich, J. Catal. 98, 102, (1986)
6. F. J. Farrell, V. A. Maroni, and T. G. Spiro, Inorganic Chemistry 8(12), 2638, (1969)
7. R.S. Tobias, Can. J. Chem. 43, 1222, (1965)
8. C. Rocchiccioli-Deltcheff, R. Thouvenot, and M. Dabbabi, Spectrochimica Acta 33A, 143, (1977)
9. W. P. Griffith, and T. D. Wickins, J. Chem. Soc. (A), 590, (1967)
10. J. E. Guerchais, and B. Spinner, Bull. Soc. Chim. France, 1122, (1965)

11. E. M. Zhurenkov, and N. Pobezhimovskaya, Radiokhimiya 12(1), 105, (1970)
12. C. Djordjevic, H. Gorican, and S. L. Tan, J. Less-Common Metals II, 342, (1966)
13. Z. X. Liu, Z. D. Lin, H. J. Fan, and F. H. Li, Appl. Phys. A 45, 159, (1988)
14. W. S. Milliam, K. I. Segawa, D. Smrz, and W. K. Hall, Polyhedron 5, 169, (1986)
15. C. L. O'Young, C. H. Yang, S. J. DeCanio, M. S. Patel, and D. A. Storm, J. Catal. 113, 307, (1988)

RECEIVED May 9, 1990